

CAST solar axion search with ^3He buffer gas: Closing the hot dark matter gap

M. Arik,^{1,*} S. Aune,² K. Barth,³ A. Belov,⁴ S. Borghi,^{3,†} H. Bräuninger,⁵ G. Cantatore,⁶ J. M. Carmona,⁷ S. A. Cetin,¹ J. I. Collar,⁸ E. Da Riva,³ T. Dafni,^{7,‡} M. Davenport,³ C. Eleftheriadis,⁹ N. Elias,^{3,§} G. Fanourakis,¹⁰ E. Ferrer-Ribas,² P. Friedrich,⁵ J. Galán,^{7,2} J. A. García,⁷ A. Gardikiotis,¹¹ J. G. Garza,⁷ E. N. Gazis,¹² T. Geralis,¹⁰ E. Georgiopoulou,¹¹ I. Giomataris,² S. Gninenko,⁴ H. Gómez,^{7,¶} M. Gómez Marzoa,^{3,**} E. Gruber,¹³ T. Guthörl,¹³ R. Hartmann,^{14,††} S. Hauf,^{15,‡‡} F. Haug,³ M. D. Hasinoff,¹⁶ D. H. H. Hoffmann,¹⁵ F. J. Iguaz,^{7,2} I. G. Irastorza,⁷ J. Jacoby,¹⁷ K. Jakovčić,¹⁸ M. Karuza,^{6,§§} K. Königsmann,¹³ R. Kotthaus,¹⁹ M. Krčmar,¹⁸ M. Kuster,^{5,15,‡‡} B. Lakić,¹⁸ P. M. Lang,¹⁵ J. M. Laurent,³ A. Liolios,⁹ A. Ljubičić,¹⁸ V. Lozza,⁶ G. Luzón,⁷ S. Neff,¹⁵ T. Niinikoski,^{3,¶¶} A. Nordt,^{5,15,§} T. Papaevangelou,² M. J. Pivovarov,²⁰ G. Raffelt,¹⁹ H. Riege,¹⁵ A. Rodríguez,⁷ M. Rosu,¹⁵ J. Ruz,^{3,20} I. Savvidis,⁹ I. Shilon,^{7,3,***} P. S. Silva,³ S. K. Solanki,^{21,†††} L. Stewart,³ A. Tomás,⁷ M. Tsagri,^{11,3} K. van Bibber,^{20,‡‡‡} T. Vafeiadis,^{3,9,11} J. Villar,⁷ J. K. Vogel,^{13,20} S. C. Yildiz,^{1,*} and K. Zioutas^{3,11}

(CAST Collaboration)

¹*Dogus University, Istanbul, Turkey*

²*IRFU, Centre d'Études Nucléaires de Saclay (CEA-Saclay), Gif-sur-Yvette, France*

³*European Organization for Nuclear Research (CERN), Genève, Switzerland*

⁴*Institute for Nuclear Research (INR), Russian Academy of Sciences, Moscow, Russia*

⁵*Max-Planck-Institut für Extraterrestrische Physik, Garching, Germany*

⁶*Instituto Nazionale di Fisica Nucleare (INFN), Sezione di Trieste and Università di Trieste, Trieste, Italy*

⁷*Instituto de Física Nuclear y Altas Energías, Universidad de Zaragoza, Zaragoza, Spain*

⁸*Enrico Fermi Institute and KICP, University of Chicago, Chicago, IL, USA*

⁹*Aristotle University of Thessaloniki, Thessaloniki, Greece*

¹⁰*National Center for Scientific Research "Demokritos", Athens, Greece*

¹¹*Physics Department, University of Patras, Patras, Greece*

¹²*National Technical University of Athens, Athens, Greece*

¹³*Albert-Ludwigs-Universität Freiburg, Freiburg, Germany*

¹⁴*MPI Halbleiterlabor, München, Germany*

¹⁵*Technische Universität Darmstadt, IKP, Darmstadt, Germany*

¹⁶*Department of Physics and Astronomy, University of British Columbia, Vancouver, Canada*

¹⁷*Johann Wolfgang Goethe-Universität, Institut für Angewandte Physik, Frankfurt am Main, Germany*

¹⁸*Rudjer Bošković Institute, Zagreb, Croatia*

¹⁹*Max-Planck-Institut für Physik (Werner-Heisenberg-Institut), München, Germany*

²⁰*Lawrence Livermore National Laboratory, Livermore, CA, USA*

²¹*Max-Planck-Institut für Sonnensystemforschung, Katlenburg-Lindau, Germany*

The CERN Axion Solar Telescope (CAST) has finished its search for solar axions with ^3He buffer gas, covering the search range $0.64\text{ eV} \lesssim m_a \lesssim 1.17\text{ eV}$. This closes the gap to the cosmological hot dark matter limit and actually overlaps with it. From the absence of excess X-rays when the magnet was pointing to the Sun we set a typical upper limit on the axion-photon coupling of $g_{a\gamma} \lesssim 3.3 \times 10^{-10}\text{ GeV}^{-1}$ at 95% CL, with the exact value depending on the pressure setting. Future direct solar axion searches will focus on increasing the sensitivity to smaller values of $g_{a\gamma}$, for example by the currently discussed next generation helioscope IAXO.

PACS numbers: 95.35.+d, 14.80.Mz, 07.85.Nc, 84.71.Ba

Introduction.—The most promising method to search for axions and axion-like particles (ALPs) [1–4], low-mass bosons with a two-photon interaction vertex, is their conversion to photons in macroscopic magnetic fields [5–7]. This approach includes the search for solar axions by the helioscope technique [8–15], photon regeneration experiments (“shining light through a wall”) [16–18], axion-photon conversion in astrophysical B fields [19–22], and the search for galactic axion dark matter [23–27].

One limiting factor in any of these efforts is the momentum difference between freely propagating photons and axions caused by the axion mass m_a . It limits the

magnetic field volume over which the conversion is coherent. In solar axion searches one can extend the search to larger m_a values by providing the photons with a refractive mass [28]. The conversion pipe is filled with a low- Z buffer gas; the search mass is chosen by adjusting the gas pressure. In this way, the CERN Axion Solar Telescope (CAST), the largest axion helioscope to date, has successively pushed its search range to higher m_a values (see Fig. 1 for a summary of results). We here report on the final search range based on ^3He buffer gas.

Within the ALP family of hypothetical bosons, the original axion is the best-motivated case because it

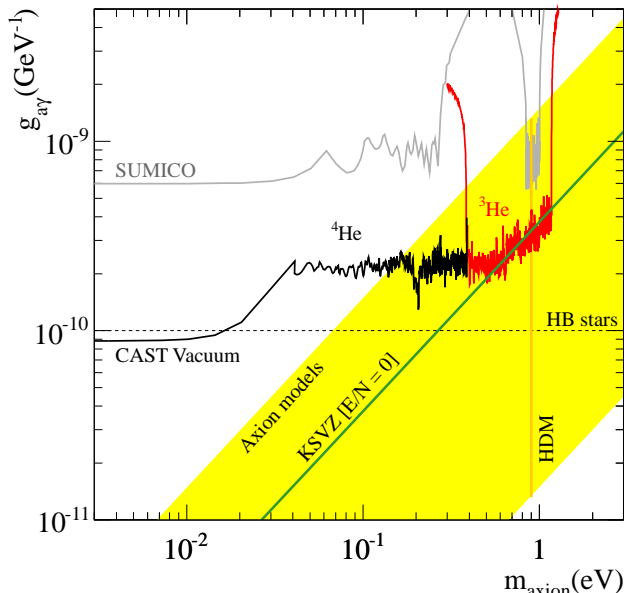


FIG. 1: Exclusion regions in the m_a - $g_{a\gamma}$ -plane achieved by CAST in the vacuum [12, 13], ^4He [14], first part of the ^3He phase [15] and our new results (all in red). We also show constraints from Sumico [9–11], horizontal branch (HB) stars [29] (a somewhat more restrictive limit stems from blue-loop suppression in massive stars [30]), and the hot dark matter (HDM) bound [31]. The yellow band represents typical theoretical models with $|E/N - 1.95| = 0.07$ – 7 . The green solid line corresponds to $E/N = 0$ (KSVZ model).

emerges from the compelling Peccei-Quinn mechanism to explain the absence of CP-violating effects in QCD. In the two-dimensional $g_{a\gamma}$ - m_a ALP parameter space, the QCD axion must lie somewhere on the line $g_{a\gamma} \propto m_a$ which is anchored to π^0 . After allowing for model-dependent numerical factors, the axion may be found anywhere in the yellow band indicated in Fig. 1. The CAST vacuum result ($g_{a\gamma} < 0.88 \times 10^{-10} \text{ GeV}^{-1}$ at 95% CL for $m_a \lesssim 0.02 \text{ eV}$ [13]) remains a milestone in the ALP landscape. However, a major objective of CAST has been to find or exclude QCD axions and thus to push as far as possible to higher m_a values. Our first ^3He limits [15] have for the first time crossed the axion line appropriate for the KSVZ model (Fig. 1) [32, 33].

QCD axions with parameters in this range thermalize in the early universe after the QCD phase transition by interactions with pions [34] and would thus exist with a present-day number density of around 50 cm^{-3} , comparable to 0.5 neutrino species, and thus are susceptible to hot dark matter bounds [31, 35, 36]. Assuming neutrino masses to be negligible, the latest axion hot dark matter bound is $m_a \lesssim 0.9 \text{ eV}$, leaving a small gap to our earlier ^3He search range which we now close.

The recent Planck measurements of the cosmic microwave background (CMB) significantly improve our

knowledge of many cosmological parameters. In contrast to earlier CMB results, Planck alone now constrains the axion mass and provides a limit $m_a < 1.01 \text{ eV}$ (95% CL). The inclusion of other data sets, notably the matter power spectrum and the HST measurement of the Hubble parameter, have only a small impact, providing limits between 0.67 and 0.86 eV, depending on the combination of data sets [37]. In other words, concerning a possible axion hot dark matter contribution to the universe, the situation after Planck is almost the same as before.

Data taking strategy.—CAST uses an LHC test dipole magnet ($L = 9.26 \text{ m}$, $B \sim 9.0 \text{ T}$) mounted on a movable platform to follow the Sun for about 1.5 h both at sunrise and sunset. One of the apertures of the magnet is covered by a CCD/Telescope system [38] and the other three by three Micromegas detectors of the microbulk type [39–42].

The axion-photon conversion probability when the conversion volume is filled with a buffer gas (^3He in our case) is

$$P_{a \rightarrow \gamma} = \left(\frac{Bg_{a\gamma}}{2} \right)^2 \frac{1 + e^{-\Gamma L} - 2e^{-\Gamma L/2} \cos(qL)}{q^2 + \Gamma^2/4} \quad (1)$$

where Γ is the inverse photon absorption length in the buffer gas, and the axion-photon momentum transfer provided by the magnetic field is $q = |m_a^2 - m_\gamma^2|/2E$. The maximum conversion probability is reached for $m_a \simeq m_\gamma$ where m_γ is the photon refraction mass which depends on the buffer gas density. For $m_a \neq m_\gamma$, the probability rapidly decreases due to the axion-photon momentum mismatch.

Throughout CAST Phase II, the data taking strategy was to increase the density in the cold bore circuit in small steps chosen to partially overlap the intrinsic mass acceptance ($\sim 1 \text{ meV}$ FWHM) of the previous setting and so scan smoothly over the whole available mass range. The original step size and exposure time have been modified on a number of occasions in order to complete the physics program more efficiently without compromising continuity, but at the expense of reduced sensitivity at higher masses.

The central gas density inside the cold bore, with the magnet horizontal, was calculated from the cold bore pressure (P_{cb}) measured at one end of the cold bore, the magnet temperature T_{mag} and the equation of state (EoS) of ^3He gas [43]. During solar tracking, P_{cb} changed continuously due to the changing hydrostatic pressure of the ^3He gas column and due to a slow characteristic temperature transient in the magnet (10–15 mK) caused by the tilting affecting the regulation and efficiency of the 1.8 K heat exchanger. In addition, because of the presence of short warm link regions, ^3He temperature and density are not uniform in the system and regions with lighter vapour are present at the extremities, where

buoyancy-driven flows occur. The magnet tilting affects such phenomena, giving rise to a redistribution of the ^3He mass and a consequent further pressure change. Computational Fluid Dynamics (CFD) simulations are required to describe the complex fluid dynamics involved which results in the measured pressure and the density profile along the cold bore.

The actual density profile cannot be measured directly but the experimental pressure variation on tilting is a key indicator which the CFD simulation must reproduce. An extensive and on-going program of CFD simulations has been undertaken. The CFD simulations take into account all requisite physical phenomena, such as gravity, natural convection and turbulence together with the geometry of the cold bores, link volumes and the cold windows and the buffer gas EoS. The boundary conditions are defined by the number of moles of ^3He gas in the system, T_{mag} and several temperatures measured around the link volumes and cold windows.

The predicted pressure variations are in satisfactory agreement with those observed experimentally when tilting [46]. This result justifies the method used in the data analysis for calculating the central density during tracking, where we use a continuously re-evaluated value for the central density, calculated from P_{cb} , the hydrostatic correction, T_{mag} and the EoS.

The density profiles derived from the CFD simulations made with the magnet horizontal and over the full range of Phase II density settings were subjected to a simple and conservative coherence criterion ($\Delta\rho < 0.001 \text{ kg m}^{-3}$). The resulting dependence of the effective coherence length L_{eff} with density was parametrised and applied to all data independent of photon energy and tilt angle. L_{eff} decreases from about $\sim 9 \text{ m}$ to $\sim 6 \text{ m}$ in the range $m_a=0.4 \text{ eV}$ to $m_a=1.15 \text{ eV}$, compared with the magnetic length of 9.26 m . The CFD simulations made with magnet tilted allow an estimate to be made that the final effect on the limit on the $g_{a\gamma}$ from applying this simple criterion to be well below 10%.

Data analysis and results.—The data presented in this paper correspond to 1100 hour \times detector taken by the three Micromegas detectors from 2009 to 2011 with ^3He in the system in axion-sensitive conditions (i.e. with the magnet tracking the Sun). Background levels are determined from a larger body of data taken during non tracking time. The data acquired by the CCD/Telescope of this period is under analysis and will be presented in a later publication. The present data correspond to about 418 effective axion mass steps that, together with the first 252 ^3He steps already released in a previous paper [15], continuously cover an axion mass range between 0.39 eV and 1.17 eV . Due to the density excursions experienced during a single tracking, data from each actual density step contribute to the neighbouring mass steps, specially for the larger densities used. The effective average exposure time per mass step is approximately 0.75 h per

detector for masses from 0.64 eV to 1 eV , while it was reduced to $\sim 0.4 \text{ h}$ per detector for masses above 1 eV .

The data analysis is performed in a manner similar to our previous results [12–15]. We use an unbinned likelihood function that can be expressed as

$$\log \mathcal{L} \propto -R_T + \sum_i^N \log R(t_i, E_i, d_i). \quad (2)$$

Here R_T is the integrated expected number of counts over all exposure time, energy and detectors. The sum runs over each of the N detected counts for the event rate $R(t_i, E_i, d_i)$ expected at the time t_i , energy E_i and detector d_i of the event i

$$R(t, E, d) = B_d + S(t, E, d), \quad (3)$$

where B_d is the background rate of detector d . $S(t, E, d)$ is the expected rate from axions in detector d which depends on the axion properties $g_{a\gamma}$ and m_a

$$S(t, E, d) = \frac{d\Phi_a}{dE} P_{a\rightarrow\gamma} \epsilon_d, \quad (4)$$

where $P_{a\rightarrow\gamma}$ is the axion photon conversion probability in the CAST magnet given by Eq. (1) and ϵ_d the detector effective area. Finally, the solar axion spectrum is

$$\frac{d\Phi_a}{dE} = 6.02 \times 10^{10} g_{10}^2 \frac{E^{2.481}}{e^{E/1.205}} \text{ cm}^{-2} \text{ s}^{-1} \text{ keV}^{-1} \quad (5)$$

with $g_{10} = g_{a\gamma}/(10^{-10} \text{ GeV}^{-1})$ and energies in keV.

As explained in [14], the m_a dependence of the above expression is encoded in the probability $P_{a\rightarrow\gamma}$, which is coherently enhanced for values of m_a matching the refractive photon mass m_γ induced by the buffer gas density, while it is negligible for values away from m_γ . Therefore, only the counts observed with the gas density matching a given axion mass m_a will contribute to $\log \mathcal{L}$ (and the exclusion plot) for that mass m_a . We stress that the value of m_γ to be introduced is time-dependent even within a single density step, due to the pressure excursions explained above.

Maximization of \mathcal{L} (for a fixed value of m_a) leads to a best-fit value of g_{min}^4 . The obtained value is compatible with the absence of a signal in the entire mass range, and therefore an upper limit on g_{95}^4 is obtained by integration of the Bayesian probability from zero up to 95% of its area in g^4 . This is computed for many values of the axion mass m_a in order to configure the full exclusion plot shown in Fig. 1. A close up of the same exclusion plot is shown in Fig. 2, focused specifically in the axion mass range which has been explored in the data presented here.

As can be seen in Fig. 1, CAST extends its previous range towards higher axion masses, excluding the interval $0.64\text{--}1.17 \text{ eV}$ down to an average value of the axion-photon coupling of $3.3 \times 10^{-10} \text{ GeV}^{-1}$. The actual

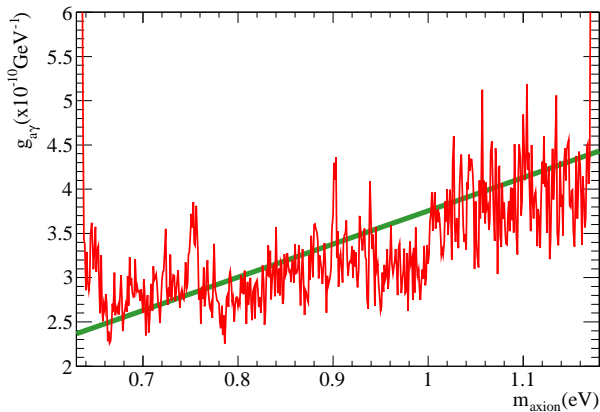


FIG. 2: Expanded view of the limit achieved in the CAST ${}^3\text{He}$ phase for the axion mass range between 0.64 eV and 1.17 eV, which corresponds to a pressure scan in ${}^3\text{He}$ from 36 mbar to 105 mbar approximately. The actual limit contour has a high-frequency structure that is a result of statistical fluctuations that occur when a limit is computed for a specific mass using only a few hours of data. The green solid line corresponds to $E/N = 0$ (KSVZ model).

limit contour has a high-frequency structure that is a result of statistical fluctuations that occur when a limit is computed for a specific mass using only a few hours of data. The apparent slope upwards in the exclusion line for higher axion masses is due to the reduction of the exposure time per density step, for $m_a > 1$ eV, as well as to the continuous decrease of L_{eff} and the increase of Γ for higher gas densities. Eventually, with the addition of the data from the CCD/Telescope system, these numbers will likely improve.

Conclusions.—CAST has finished its phase of using ${}^3\text{He}$ buffer gas, continuing the search to its limiting pressure setting corresponding to a search mass of $m_a = 1.17$ eV. In this way, the search range now generously overlaps with the current cosmic hot dark matter bound of $m_a \lesssim 0.9$ eV and there would be little benefit in pushing to yet larger masses with the buffer-gas technique. CAST has not found axions and the next challenge is to move down in the m_a - g_{ar} plot to reach the “axion band” of theoretical models in a broader range of masses. Such a goal cannot be achieved with the existing CAST apparatus and will require significant improvements of detector and magnet properties, such as the proposed International AXion Observatory (IAXO) [44, 45] or a completely new approach.

Acknowledgments.—We thank CERN for hosting the experiment and for the technical support to operate the magnet and cryogenics. We thank the CERN CFD team for their essential contribution to the CFD work. We acknowledge support from NSERC (Canada), MSES (Croatia) under the grant number 098-0982887-2872, CEA (France), BMBF (Germany) under the grant num-

bers 05 CC2EEA/9 and 05 CC1RD1/0 and DFG (Germany) under grant numbers HO 1400/7-1 and EXC-153, the Virtuelles Institut für Dunkle Materie und Neutrinos VIDMAN (Germany), GSRT (Greece), RFFR (Russia), the Spanish Ministry of Economy and Competitiveness (MINECO) under grants FPA2008-03456 and FPA2011-24058, partially funded by the European Regional Development Fund (ERDF/FEDER), the European Research Council (ERC) under grant ERC-2009-StG-240054 (T-REX), Turkish Atomic Energy Authority (TAEK), NSF (USA) under Award number 0239812, US Department of Energy, NASA under the grant number NAG5-10842. Part of this work was performed under the auspices of the US Department of Energy by Lawrence Livermore National Laboratory under Contract DE-AC52-07NA27344. We acknowledge the helpful discussions within the network on direct dark matter detection of the ILIAS integrating activity (Contract number: RII3-CT-2003-506222).

-
- * Present addr.: Bogazici University, Istanbul, Turkey.
 - † Present addr.: School of Physics and Astronomy, Schuster Laboratory, University of Manchester, Manchester, UK.
 - ‡ Corresponding author: Theopisti.Dafni@unizar.es
 - § Present addr.: European Spallation Source ESS AB, Lund, Sweden.
 - ¶ Present addr.: Laboratoire de l’Accélérateur Linéaire (LAL), Orsay, France.
 - ** Also at.: Laboratoire de Transfert de Chaleur et de Masse, École Polytechnique Fédérale de Lausanne (EPFL), Lausanne, Switzerland.
 - †† Present addr.: PNSensor GmbH, München, Germany.
 - ‡‡ Present addr.: European XFEL GmbH, Notkestrasse 85, 22607 Hamburg, Germany.
 - §§ Present addr.: Physics Department and Center for Micro and Nano Sciences and Technologies, University of Rijeka, Croatia.
 - ¶¶ Present addr.: Excellence Cluster Universe, Technische Universität München, Garching, Germany.
 - *** Also at.: Physics Department, Ben-Gurion University of the Negev, Beer-Sheva 84105, Israel.
 - ††† Sec. Affiliation: School of Space Research, Kyung Hee University, Yongin, Republic of Korea.
 - ‡‡‡ Present addr.: University of California Berkeley, CA, USA.
- [1] J. Jaeckel and A. Ringwald, *Ann. Rev. Nucl. Part. Sci.* **60**, 405 (2010).
 - [2] A. Ringwald, *Phys. Dark Univ.* **1**, 116 (2012).
 - [3] J. L. Hewett *et al.*, arXiv:1205.2671.
 - [4] P. Brun, arXiv:1304.1330
 - [5] P. Sikivie, *Phys. Rev. Lett.* **51**, 1415 (1983); (E) *ibid.* **52**, 695 (1984).
 - [6] G. Raffelt and L. Stodolsky, *Phys. Rev. D* **37**, 1237 (1988).
 - [7] S. J. Asztalos *et al.*, *Ann. Rev. Nucl. Part. Sci.* **56**, 293 (2006).
 - [8] D. M. Lazarus *et al.*, *Phys. Rev. Lett.* **69**, 2333 (1992).

- [9] S. Moriyama *et al.*, Phys. Lett. B **434**, 147 (1998).
- [10] Y. Inoue *et al.*, Phys. Lett. B **536**, 18 (2002).
- [11] Y. Inoue *et al.*, Phys. Lett. B **668**, 93 (2008).
- [12] K. Zioutas *et al.* (CAST Collaboration), Phys. Rev. Lett. **94**, 121301 (2005).
- [13] S. Andriamonje *et al.* (CAST Collaboration), JCAP **0704**, 010 (2007).
- [14] E. Arik *et al.* (CAST Collaboration), JCAP **0902**, 008 (2009).
- [15] M. Arik *et al.* (CAST Collaboration), Phys. Rev. Lett. **107**, 261302 (2011).
- [16] K. Van Bibber *et al.*, Phys. Rev. Lett. **59**, 759 (1987).
- [17] J. Redondo, A. Ringwald and , Contemp. Phys. **52**, 211 (2011).
- [18] R. Bähre *et al.*, arXiv:1302.5647.
- [19] A. Payez, J. R. Cudell and D. Hutsemekers, JCAP **1207**, 041 (2012).
- [20] A. De Angelis, G. Galanti and M. Roncadelli, Phys. Rev. D **84**, 105030 (2011).
- [21] D. Horns, L. Maccione, M. Meyer, A. Mirizzi, D. Montanino and M. Roncadelli, Phys. Rev. D **86**, 075024 (2012).
- [22] M. Meyer, D. Horns and M. Raue, Phys. Rev. D **87**, **035027** (2013).
- [23] S. J. Asztalos *et al.* (ADMX Collaboration), Phys. Rev. Lett. **104**, 041301 (2010).
- [24] J. Hoskins *et al.*, Phys. Rev. D **84**, 121302 (2011).
- [25] S. J. Asztalos *et al.*, Nucl. Instrum. Meth. A **656**, 39 (2011).
- [26] O. K. Baker *et al.*, Phys. Rev. D **85**, 035018 (2012).
- [27] D. Horns *et al.*, JCAP **1304**, 016 (2013).
- [28] K. van Bibber, P. M. McIntyre, D. E. Morris and G. G. Raffelt, Phys. Rev. D **39**, 2089 (1989).
- [29] G. G. Raffelt, Lect. Notes Phys. **741**, 51 (2008).
- [30] A. Friedland, M. Giannotti and M. Wise, Phys. Rev. Lett. **110**, 061101 (2013).
- [31] S. Hannestad, A. Mirizzi, G. G. Raffelt and Y. Y. Y. Wong, JCAP **1008**, 001 (2010).
- [32] J. E. Kim, Phys. Rev. Lett. **43**, 103 (1979).
- [33] M. A. Shifman, A. I. Vainshtein and V. I. Zakharov, Nucl. Phys. B **166**, 493 (1980).
- [34] S. Chang and K. Choi, Phys. Lett. B **316**, 51 (1993).
- [35] S. Hannestad, A. Mirizzi and G. Raffelt, JCAP **0507**, 002 (2005).
- [36] A. Melchiorri, O. Mena and A. Slosar, Phys. Rev. D **76**, 041303 (2007).
- [37] M. Archidiacono, S. Hannestad, A. Mirizzi, G. Raffelt and Y. Y. Y. Wong, arXiv:1307.0615.
- [38] M. Kuster *et al.*, New J. Phys. **9**, 169 (2007).
- [39] P. Abbon *et al.*, New J. Phys. **9**, 170 (2007).
- [40] S. Andriamonje *et al.*, JINST **5**, P02001 (2010).
- [41] J. Galan *et al.*, JINST **5**, P01009 (2010).
- [42] S. Aune *et al.* (CAST Collaboration), Nucl. Instrum. Meth. A **604**, 15 (2009).
- [43] E. W. Lemmon (NIST), private communication.
- [44] I. G. Irastorza *et al.*, JCAP **1106**, 013 (2011).
- [45] I. Shilon, A. Dudarev, H. Silva and H. H. J. ten Kate, IEEE T Appl. Supercon. **23**, 3, p. 4500604 (2013).
- [46] The technical details of these simulations and the comparison with observations will be the subject of a detailed future paper.